Eur. Phys. J. B **32**, 181–187 (2003)
DOI: 10.1140/epjb/e2003-00087-5

THE EUROPEAN PHYSICAL JOURNAL B

Electron-phonon interaction in carbon schwarzites

I. Spagnolatti, M. Bernasconi[a], and G. Benedek

Dipartimento di Scienza dei Materiali and Istituto Nazionale per la Fisica della Materia, Università degli Studi di Milano-Bicocca, Via Cozzi 53, 20125 Milano, Italy

Received 19 December 2002
Published online 1st April 2003 –

Abstract. The recent synthesis of random schwarzites has stimulated the present *ab initio* calculation of the electronic structure and electron-phonon interaction in two different periodic D-type schwarzites, fcc-$(C_{28})_2$ (made of 24 seven-membered rings per unit cell) and fcc-$(C_{64})_2$ (made of 12 eight membered and 48 six-membered rings per unit cell). Like in fullerenes, also in schwarzites the electron-phonon interaction potential is found to increase with the absolute Gauss curvature, though it remains smaller than for doped fullerenes.

PACS. 71.15.Mb Density functional theory, local density approximation, gradient and other corrections – 74.70.Wz Fullerenes and related materials – 74.10.+v Occurrence, potential candidates

1 Introduction

The discovery of high superconducting transition temperature in alkali-doped C_{60} (T_c = 10−40 K) has attracted much attention on carbon-based materials as a possible new class of superconductors [1,2]. Although the origin of superconductivity in C_{60} is still controversial, it is generally accepted that a large electron-phonon coupling plays a crucial role in providing a high T_c. The electron-phonon coupling is stronger in C_{60} with respect, for instance, to graphite because of the large curvature of the graphene structure of the cluster [3]. Smaller fullerenes (C_{36}, C_{28}, C_{20}) with a larger curvature have been predicted to have larger electron-phonon coupling [4–8]. Possible solid forms of C_{36} [7] and C_{20} [8] have been also proposed recently. Fullerenes are one of the ways in which curvature can be introduced into a graphitic net. An alternative class of structures, known as schwarzites, have been proposed theoretically [9–12,14]. These structures have a negative Gaussian curvature associated with the presence of seven- or eight-membered rings, in contrast to fullerenes which have a positive Gaussian curvature due to the presence of five-membered rings. As in fullerenes, all atoms in schwarzites are three-fold coordinated. The recent synthesis of a spongy form of carbon with the structure of a random schwarzite [15] has stimulated the present *ab initio* study of the electron-phonon interaction in periodic schwarzites. Special attention is given to the dependence of the electron-phonon coupling on the Gaussian curvature and its role in their potential superconductive properties.

[a] e-mail: marco.bernasconi@unimib.it

Although periodic schwarzites have not been realized experimentally so far, there is clear evidence that random schwarzites in the form of highly porous, nanostructured carbon are produced by cluster assembling in films deposited by pulsed microplasma cluster sources [15]. Periodic schwarzites, however, are obviously more suitable to be studied theoretically by *ab initio* methods. We have thus confined ourselves to study the structural, electronic and vibrational properties of two periodic D-type schwarzites with a face-centered-cubic structure, fcc-$(C_{28})_2$ (with 56 atoms per unit cell) and fcc-$(C_{64})_2$ (with 128 atoms per unit cell). The calculations have been performed within density functional theory in the local density approximation, with norm-conserving pseudopotential and plane wave expansion of the Kohn-Sham orbitals up to a kinetic cutoff of 40 Ry, as implemented in the code CPMD [16,17]. The topological properties which have been used to build the two crystals fcc-$(C_{28})_2$ and fcc-$(C_{64})_2$ are briefly reviewed in the next section. The results on the structural, electronic, and vibrational properties and on the electron-phonon coupling are reported below for each crystal in Sections 3 and 4.

2 Topological properties of schwarzites

Periodic schwarzites are generated by covalent connection of identical elements. The unit cell may contain one or more such elements. The centers of the elements can be seen as the nodes of a dual lattice. The diamond structure is a possible dual lattice which defines an important class of cubic schwarzites, with two elements per unit cell (*bi-elemental* schwarzites), each element being 4-fold

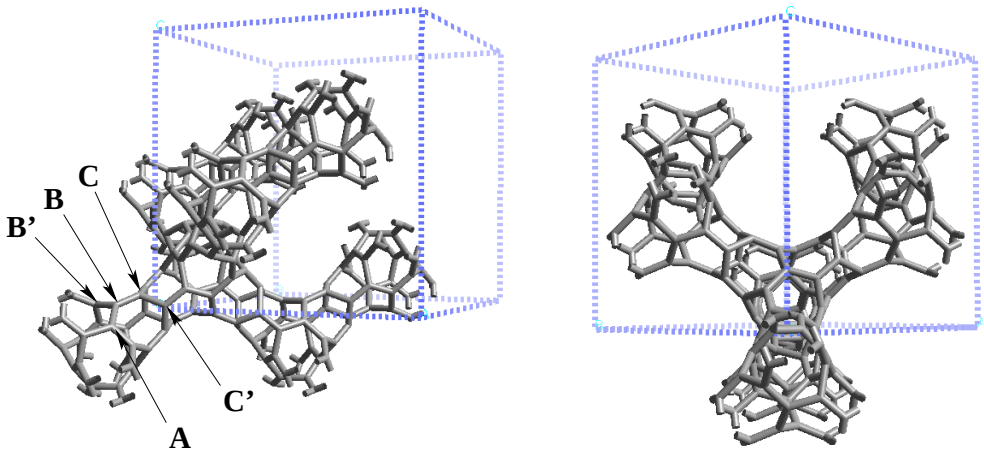

Fig. 1. The face-centered-cubic structure of the schwarzite fcc-$(C_{28})_2$. The conventional unit cell with four formula units is shown. The coordinates of the three independent atoms (A, B, C) are given in the text. Atom C' (B') is obtained from C (B) by applying a symmetry operation.

coordinated with neighboring elements. These structures are tessellations of a D-type Schwarz minimal surface [9]. *Mono-elemental* cubic schwarzites with a *sc*, *bcc* or *fcc* dual lattices are also possible, though the negative curvature of the elements becomes large, due to the increased coordination (6, 8 and 12, respectively for *sc*, *bcc*, and *fcc*), and energetically unfavorable. However, *sc* (P-type) carbon schwarzites of the polybenzene family have been predicted to be rather stable [12].

The topology of schwarzites can be explained starting from the Euler's theorem [18] for the polygonal tiling of a surface, analogously to the treatment of fullerenes. Since schwarzites are open, infinitely extending surfaces, Euler's theorem will refer to the unit cell. In D-type schwarzites each element is linked to four identical elements and has tetrahedral symmetry and four open terminations. Correspondingly, the unit cell containing two joint elements has six terminations. From the topological point of view it can be closed on itself by (ideally) joining three pairs of opposite terminations, this operation being equivalent to the cyclic boundary conditions for the periodic crystal. This closure procedure transforms the unit cell into a three-hole torus, characterized by a connection order per unit cell $K_{uc} = 7$ [9] or a single element into a two-hole torus with a connection order per element $K_{el} = 5$. Thus the polygonal tiling of a D-type surface must obey the Euler's law per element in the form $\nu_{el} - e_{el} + f_{el} = 3 - K_{el} = -2$, where ν_{el}, e_{el} and f_{el} are the numbers of vertices (atoms), edges (bonds) and polygonal faces (rings) per element.

The tiling with only one kind of polygons (*minimal or Platonic tiling*) leads to well defined numbers of polygons. In all cases, the polygons cannot be other than heptagons, octagons or ennagons. Each minimal tiling is the zeroth element of an infinite series of larger schwarzites obtained by inserting in each element a number of hexagons. The zeroth elements of the three series contain, respectively, 12 heptagons, 6 octagons and 4 ennagons per element. The corresponding smallest D-type schwarzites will therefore have 56, 32 and 24 atoms per unit cell. The number of hexagons that can be added to obtain larger D-type schwarzites is not arbitrary, but fixed by the request that the tetrahedral symmetry is preserved.

In this work we consider two D-type schwarzites. Firstly, the smallest schwarzite of the heptagonal class, fcc-$(C_{28})_2$ which is the counterpart of the fullerene C_{20} and will allow us to compare the main properties of these two systems as representative of two different families. In fcc-$(C_{28})_2$ the elemental unit contains 28 atoms and occupies the sites of the diamond lattice (56 atoms per unit cell). Then we have considered a larger schwarzite of the octagonal class with 24 hexagons and 6 octagons (64 atoms) per unit element (fcc-$(C_{64})_2$).

3 The schwarzite fcc-$(C_{28})_2$

3.1 Structural and electronic properties

The crystal fcc-$(C_{28})_2$ is the smallest schwarzite of the heptagonal class (Fig. 1). It has a tetrahedral symmetry and can be seen as formed by C_{28} units in the sites of a diamond lattice. Each C_{28} unit contain 12 heptagons and no hexagon. The Bravais lattice is face-centered-cubic with space group $Fm\bar{3}$. We have fully optimized the structure of fcc-$(C_{28})_2$ by computing its equation of state at zero temperature (energy *versus* volume). In the total energy calculations, the integration of the Brillouin Zone (BZ) have been performed over a $4\times4\times4$ Monkhorst-Pack [19] mesh corresponding to 8 k-points in the irreducible wedge. The equation of state (Fig. 2) has been fitted by Murnaghan's function [20] which gives the lattice parameter and density ($a = 14.96$ Å, ρ=1.33 g/cm^3), bulk modulus ($B = 936$ kbar), and derivative of the bulk modulus with respect to pressure ($B' = 2.36$). The calculated cohesive energy at equilibrium is 0.771 eV/atom lower than that of diamond (the experimental cohesive energy of diamond is 7.37 eV/atom [21]).

Only three atoms out of 56 in the unit cell are inequivalent, the other being obtained by symmetry.

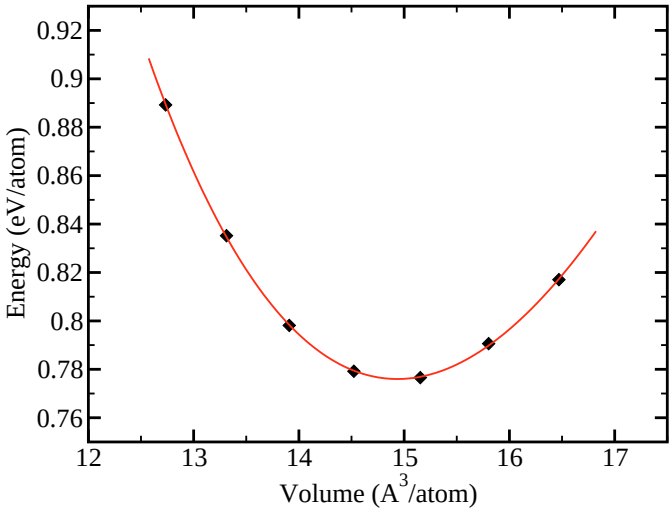

Fig. 2. Equation of state of fcc-$(C_{28})_2$. The energy zero corresponds to the total energy of diamond.

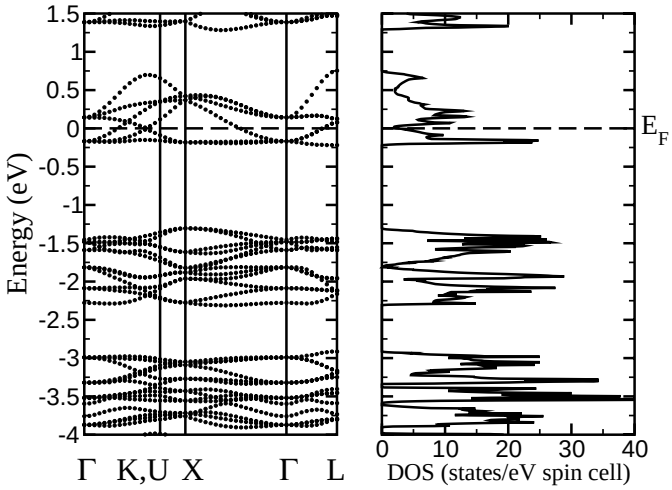

Fig. 3. Electronic band structure and density of states of the schwarzite fcc-$(C_{28})_2$. The zero of energy is the Fermi level. The density of state is computed with the tetrahedron method and 35 k-points in the irreducible BZ.

The coordinates in units of a of the inequivalent atoms labeled A, B and C in Figure 1 are $A = (-0.073, -0.302, -0.232)$, $B = (-0.200, -0.050, -0.050)$, and $C = (-0.174, -0.115, 0.018)$. There are four different bonds in the crystal, corresponding to the segments AB, BC, BB' and CC' in Figure 1. The bond BC is comparatively short (1.369 Å) whereas the other three ($AB = 1.454$ Å, $BB' = 1.498$ Å and $CC' = 1.494$ Å) are appreciably longer than the bond length in graphite (1.423 Å). Carbon schwarzites can be either metallic or insulating, depending on their atomic geometry [14]. The schwarzite fcc-$(C_{28})_2$ is metallic as shown by the electronic band structure in Figure 3.

The density of states (DOS, *cf.* Fig. 3) shows very sharp peaks due to the small dispersion of the electronic bands. The Fermi level (E_F) lies in a pseudogap of the DOS which at E_F is as low as $N(E_F) =$ 2.0 states/(eV spin cell). The lowest conduction bands correspond to p_z-states poorly conjugated localized on the atoms of CC' ring and on atom A. In particular, the lowest conduction bands are generated by two states 3-fold degenerate at Γ. They are occupied by a total number of four electrons per unit cell. The flatness of the electronic bands makes possible to restrict the BZ integration to the Γ-point only, provided that the four conduction electrons per cell are equally distributed among the lowest 3-fold degenerate conduction states at Γ (*cf.* Fig. 3). In fact, we have verified that the atomic positions do not change (within 0.005 Å) by optimization of the structure in the Γ-point approximation. The latter approximation has then been used (see next section) in the calculation of phonons and of the electron-phonon coupling.

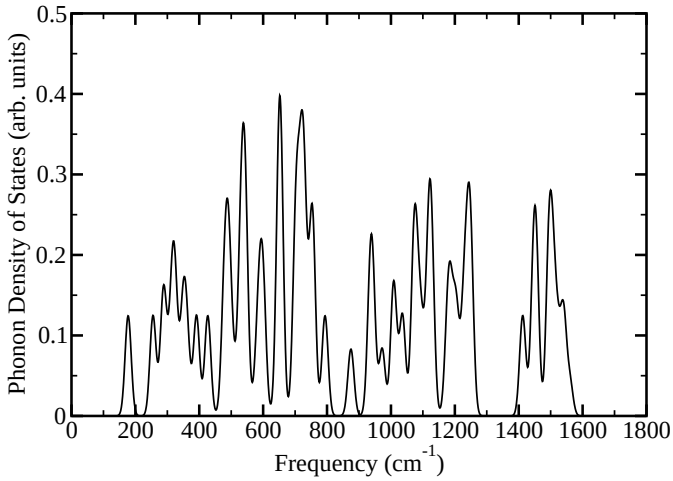

Fig. 4. Phonon density of states at the Γ-point of the schwarzite fcc-$(C_{28})_2$. The continuous line is obtained by assigning a Gaussian with variance of 15 cm^{-1} to each phonon frequency.

3.2 Phonons and electron-phonon interaction

The phonons frequencies and the eigenvectors at the Γ-point have been obtained by diagonalization of the dynamical matrix, built from the numerical derivatives of the forces with respect to finite (0.005 Å) atomic displacements. The phonon density of states at the Γ-point is reported in Figure 4. The frequency and character of the *gerade* (g), Raman-active phonons are given in Table 1. The flatness of the conduction bands at the Fermi level allows to estimate the electron-phonon coupling potential $\lambda/N(E_F)$ in the so-called molecular-approximation, which amounts to consider flat electronic and phononic bands, as

$$\frac{\lambda}{N(E_F)} = \sum_\alpha \frac{\lambda_\alpha}{N(E_F)} = \sum_\alpha \frac{1}{\omega_\alpha^2 s^2 M} \sum_{n,m}^{s} | \langle u_m \mid \epsilon_\alpha \cdot \nabla V_{\text{eff}} \mid u_n \rangle |^2, \quad (1)$$

Table 1. The contributions of the Γ-point phonons to the electron-phonon coupling constants $\lambda_\alpha/N(E_F)$ for the schwarzite fcc-$(C_{28})_2$.

Modes	Energy (cm^{-1}) fcc-$(C_{28})_2$	$\lambda_\alpha/N(0)$ (meV)
$T_g(1)$	255	1.4
$E_g(1)$	291	7.1
$T_g(2)$	314	0.1
$T_g(3)$	391	0.5
$T_g(4)$	426	4.9
$T_g(5)$	489	0.0
$A_g(1)$	493	0.4
$A_g(2)$	506	1.8
$E_g(2)$	527	3.8
$T_g(6)$	532	1.0
$T_g(7)$	544	13.8
$T_g(8)$	600	0.5
$A_g(3)$	646	0.0
$E_g(3)$	651	3.1
$T_g(9)$	653	0.0
$A_g(4)$	704	3.6
$T_g(10)$	708	0.3
$T_g(11)$	727	0.5
$T_g(12)$	753	4.2
$T_g(13)$	934	3.3
$E_g(4)$	972	1.2
$A_g(5)$	1008	0.0
$T_g(14)$	1036	0.9
$T_g(15)$	1071	0.9
$E_g(5)$	1095	1.6
$T_g(16)$	1128	0.0
$A_g(6)$	1174	0.1
$T_g(17)$	1182	0.1
$T_g(18)$	1241	0.2
$E_g(6)$	1247	0.5
$T_g(19)$	1445	0.2
$T_g(20)$	1454	0.1
$E_g(7)$	1497	0.0
$T_g(21)$	1540	0.0
$A_g(7)$	1560	0.7
Total:		**58.3**

where ϵ_α is the normalized displacement pattern of the phonon with frequency ω_α, M is the atomic mass, u_n is the periodic part of the Kohn-Sham states, and ∇V_{eff} is the derivative of the Kohn-Sham effective potential with respect to the atomic displacements caused by phonons. The sum over α and n, m run over the phonons and the s degenerate electronic states at the Fermi level at the Γ-point. The change in the effective potential due to the α-th phonon is computed by finite differences as

$$\epsilon_\alpha \cdot \nabla V_{\text{eff}} = (V_{\text{eff}}(\mathbf{r} + h\epsilon_\alpha) - V_{\text{eff}}(\mathbf{r} - h\epsilon_\alpha))/2h, \qquad (2)$$

where $h = 0.005$ Å and $\mathbf{r}$ indicate collectively the equilibrium atomic positions. Only phonons with g character contribute to the matrix elements in equation (1). The frequency and partial electron-phonon coupling constants for each normal mode are reported in Table 1.

The total electron-phonon coupling constant is $\lambda/N(E_F) = 0.058$ eV. The phonon that mostly contributes to $\lambda/N(E_F)$ is the mode $T_g(7)$ (*cf.* Tab. 1), whose displacement pattern is shown in Figure 5. This modes deforms the CC' ring over which the KS states at E_F are mostly localized. The strength of electron-phonon interaction potential in fcc-$(C_{28})_2$ is comparable to that of C_{60} fullerite ($\lambda/N(E_F) \sim 0.07$ eV in C_{60}^{3-}) [2,8], but it is substantially lower than in a C_{20}-based solid *e.g.*, the fcc-C_{22} crystal of reference [8], although the C_{20} cluster has an absolute Gaussian curvature similar to that of schwarzite fcc-$(C_{28})_2$. The schwarzite element C_{28} is actually the counterpart of C_{20} with heptagons replaced by pentagons. In this respect, we note that the large electron-phonon coupling in the C_{20}-based solid, fcc-C_{22}, is due to the phonon-induced modulation of the antibonding π-states in the short C=C ethylenic bonds, which have however a large σ-character [8]. Conversely, in fcc-$(C_{28})_2$ the states at the Fermi level are nearly p_z-states with a low σ-character and are poorly conjugated.

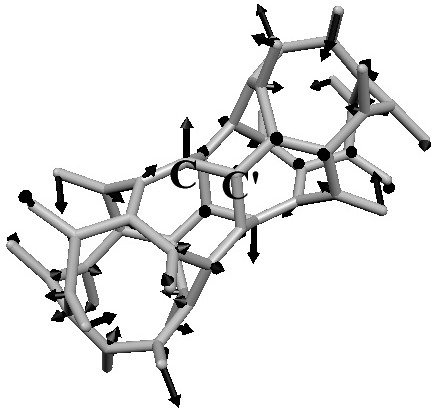

Fig. 5. Displacement pattern of the mode which gives the largest contribution to the electron-phonon coupling (see Tab. 1).

From the calculated value of $\lambda/N(E_F)$ and $N(E_F)$ we obtain λ=0.116. This value is quite low, but it could be increased by up to a factor five by increasing $N(E_F)$ *via* doping with alkali metals. The latter ions could presumably sit in the large voids of the schwarzite structure, they

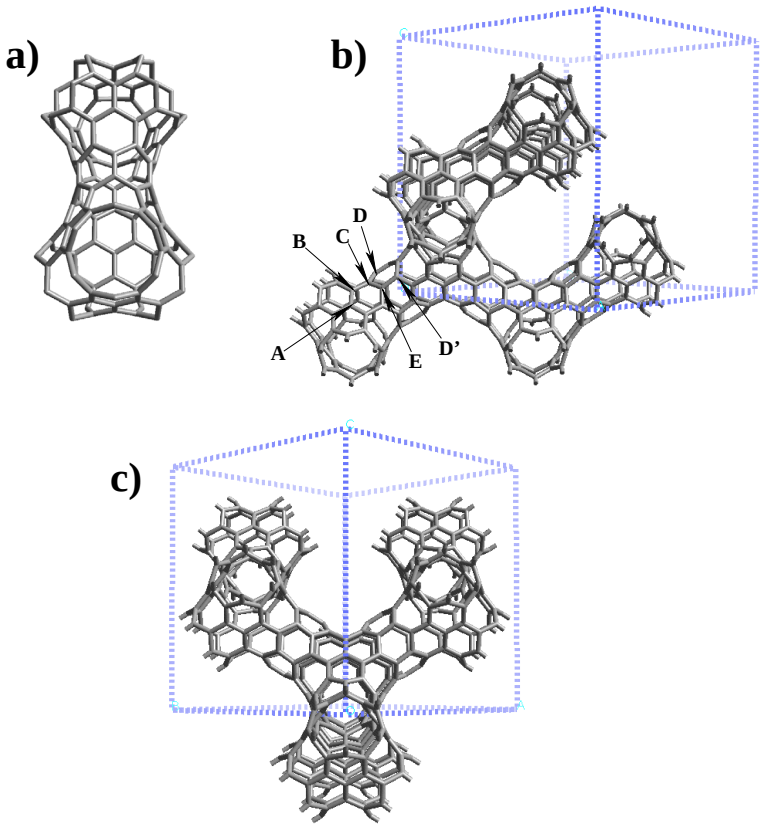

Fig. 6. (a) Basic unit of schwarzite fcc-$(C_{64})_2$ made of two elements (128 atoms). (b) Conventional unit cell of fcc-$(C_{64})_2$ with four formula units seen along the [110] and (c) [111] directions.

would get ionized and move the Fermi level at higher energy with a consequent increase of $N(E_F)$ (*cf.* Fig. 3).

4 The schwarzite fcc-$(C_{64})_2$

4.1 Structural and electronic properties

Negative curvature can be introduced in a D-type schwarzite by octagons instead of heptagons as in fcc-$(C_{28})_2$. The smallest schwarzite of the octagonal series has six octagons and 16 atoms in the elemental unit. Placing this unit on a diamond lattice gives rise to the schwarzite fcc-$(C_{16})_2$. Starting from the smallest schwarzite of this series, it is possible to make the structure bigger by inserting hexagons in such a way as to preserve the tetrahedral symmetry of the elemental unit. This is achieved by inserting hexagons in the planes perpendicular to the three-fold axis along the {111} directions. Adding one hexagon per axis one obtains the polybenzene structure studied by M. O'Keeffe *et al.* [12].

Adding three hexagons, one obtains the schwarzite fcc-$(C_{64})_2$ shown in Figure 6. There are 64 atoms per elemental unit and 128 atoms per unit cell. As for the first element of this series, the space group is $Fd\bar{3}m$. Only five atoms are inequivalent, the other being obtained by symmetry operations.

Due to the larger size of the schwarzite fcc-$(C_{64})_2$, its equation of state has been computed within the tight-binding scheme of reference [13] which has been demonstrated to reproduce the equilibrium density of several carbon-based materials including the schwarzite fcc-$(C_{28})_2$ (the latter within 0.1%). The resulting equilibrium density and lattice parameter are $\rho = 1.19$ g/cm^3 and $a = 20.45$ Å. Starting from this structure we have optimized the system at fixed volume within the *ab initio* framework. A $2 \times 2 \times 2$ MP mesh [19] has been used in the BZ integration. Residual forces at equilibrium are less than 6 mRy/bohr. Hermite-Gaussian broadening of order one with spreading of 0.04 Ry has been used to deal with metallic systems [22]. The optimized positions (*ab initio*) of the five inequivalent atoms in unit of a are (*cf.* Fig. 6) $A = (-0.2114, -0.2114, -0.2114)$, $B = (-0.1797, -0.1797, -0.2651)$, $C = (-0.2774, -0.2774, -0.1123)$, $D = (-0.1245, -0.2106, -0.2937)$, and $E = (-0.1811, -0.0688, -0.3250)$.

The bond lengths are all very similar ranging from 1.418 Å to 1.439 Å, close to the value of the bondlenghth in graphite. The cohesive energy is 0.42 eV/atom lower than that of diamond or 0.351 eV/atom higher than that of the smaller schwarzite fcc-$(C_{28})_2$, as expected due to the presence of hexagons.

The electronic band structure of fcc-$(C_{64})_2$ is reported in Figure 7. The system is a metal and the bandwidth of the lowest conduction bands is smaller than 1 eV.

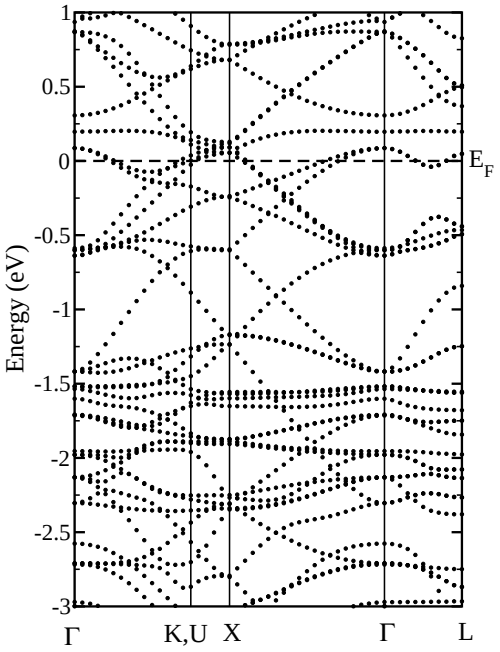

Fig. 7. Bands structure around the Fermi level of schwarzite fcc-$(C_{64})_2$. The zero of energy is the Fermi level.

As for fcc-$(C_{28})_2$, we have checked that the structure of fcc-$(C_{64})_2$ does not change by restricting the BZ integration to the Γ-point only and equally distributing the conduction electrons (two per cell) on the 2-fold degenerate state of the lowest conduction band at Γ (*cf.* Fig. 7).

4.2 Phonons and electron-phonon interaction

The phonon frequencies at the Γ-point and the electron-phonon interaction potential in the molecular-like approximation (*cf.* Eq. (1)) have been computed as described for fcc-$(C_{28})_2$ (Sect. 3). The phonon density of states at the Γ-point of fcc-$(C_{64})_2$ is shown in Figure 8.

The total electron-phonon interaction potential of schwarzite fcc-$(C_{64})_2$ is $\lambda/N(E_F) = 0.015$ eV. As expected, this value is much lower than the corresponding value in the smaller schwarzite fcc-$(C_{28})_2$, since the insertion of hexagons reduces the local curvature. Moreover the presence of octagons, which unlike heptagons in fcc-$(C_{28})_2$ have an even number of edges, increases the π-conjugation and make all the bond lengths very similar. In fcc-$(C_{64})_2$ there are no short ethylenic-like bonds as in fcc-$(C_{28})_2$.

5 Discussion and conclusions

In summary, we have reported on the first calculation of the electron-phonon interaction in carbon schwarzites. We have considered two examples of periodic scharzites of D-type: the smallest schwarzite of the series with heptagons, fcc-$(C_{28})_2$, and the schwarzite of the series with octagons which contains 24 additional hexagons per elemental unit, fcc-$(C_{64})_2$. Both schwarzites have face-centered-cubic symmetry and are metallic. The dispersion of the lowest conduction bands is low for both structures and the calculated electron-phonon interaction potential $\lambda/N(E_F)$ in the molecular-like approximation is 58 meV and 15 meV for the smaller and larger schwarzites, respectively. From these results we can conclude that also for the graphenic structure with negative curvature the same rule demonstrated for fullerenes holds, *i.e.* a large enhancement of the electron-phonon coupling can be obtained by increasing the absolute curvature. The value of $\lambda/N(E_F)$ for the smaller schwarzite is similar to that of C_{60} fullerite, but the electronic density of states is low, which finally yields $\lambda = 0.116$, a much lower value than in alkali doped C_{60}. However, $N(E_F)$ could be made larger by doping fcc-$(C_{28})_2$ with alkali metals. We note that $\lambda/N(E_F)$ is much lower in fcc-$(C_{28})_2$ than in a C_{20}-based solid (0.27 eV for the fcc-C_{22} crystal of Ref. [8]), although the C_{20} cluster has a curvature similar to fcc-$(C_{28})_2$, albeit of opposite sign. This is due to the weaker σ-character of the lowest conduction bands which contribute to the electron-phonon coupling in schwarzites. Schwarzites thus seem less attractive as potential superconductors than small fullerenes.

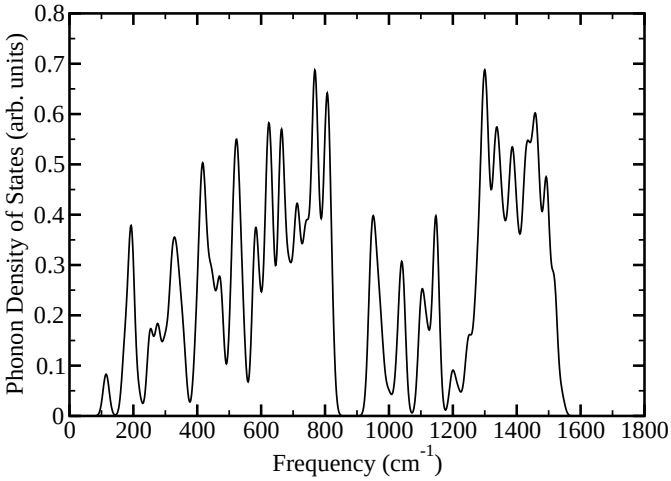

Fig. 8. Phonon density of states of schwarzite fcc-$(C_{64})_2$, from the Γ-point phonons only. The DOS is obtained by assigning a Gaussian with variance of 15 cm^{-1} to each phonon frequency.

This work is partially supported by the INFM Parallel Computing Initiative, and by MURST through project PRIN01-2001021133.

References

1. A.F. Hebard, M.J. Rosseinsky, R.C. Haddon, D.W. Murphy, S.H. Glarum, T.T.M. Palstra, A.P. Ramirez, A.R. Kortan, Nature **350**, 600 (1991)
2. O. Gunnarsson, Rev. Mod. Phys. **69**, 575 (1997)
3. M. Schluter, M. Lannoo, M. Needels, G.A. Baraff, D. Tománek, Phys. Rev. Lett. **68**, 526 (1992)
4. A. Devos, M. Lannoo, Phys. Rev. B **58**, 8236 (1998)
5. G.B. Adams, O.F. Sankey, J.B. Page, M. O'Keeffe, Chem. Phys. **176**, 61 (1993)

6. N. Breda, R.A. Broglia, G. Colò, G. Onida, D. Provasi, E. Vigezzi, Phys. Rev. B **62**, 130 (2000)
7. M. Coté , J.C. Grossman, M.L. Cohen, S.G. Louie, Phys. Rev. Lett. **81**, 697 (1998)
8. I. Spagnolatti, M. Bernasconi, G. Benedek, Europhys. Lett. **59**, 572 (2002); Z. Iqbal *et al.*, Eur. Phys. J. B **31**, 509 (2003)
9. A.L. Mackay, Nature **314**, 604 (1985)
10. D. Vanderbilt, J. Tersoff, Phys. Rev. Lett. **68**, 511 (1992)
11. A.L. Mackay, H. Terrones, Nature **352**, 762 (1991)
12. M. O'Keeffe, G.B. Adams, O.F. Sankey, Phys. Rev. Lett. **68**, 2325 (1992)
13. C.H. Xu, C.Z. Wang, C.T. Chan, K.M. Ho, J. Phys. Cond. Matt. **4**, 6047 (1992)
14. S. Gaito, L. Colombo, G. Benedek, Europhys. Lett. **44**, 525 (1998)
15. E. Barborini *et al.*, Appl. Phys. Lett. **81**, 3359 (2002)
16. CPMD version 3.0, developed by J. Hutter *et al.*, Max-Planck-Institut für Festkörperforschung and IBM Research Laboratory (1990–2001)
17. D. Marx, J. Hutter, in *Modern Methods and Algorithms of Quantum Chemistry*, edited by J. Grotendorst (John von Neumann Institute for Computing, Jülich, NIC Series, Vol. 1, 2000), pp. 301–449
18. D. Hilbert, S. Cohn-Vossen, *Anschauliche Geometrie* (Springer, Berlin) 1932
19. H.J. Monkhorst, J.D. Pack, Phys. Rev. B **13**, 5188 (1976)
20. D. Murnaghan, Proc. Nat. Acad. Sci. USA, **30**, 224 (1944)
21. M.T. Yin, M.L. Cohen, Phys. Rev. B **24**, 6121 (1981); and references therein
22. M. Methfessel, A.T. Paxton, Phys. Rev. B **40**, 3616 (1989)